Stretching single molecules into novel conformations using the atomic force microscope

Thomas E. Fisher, Piotr E. Marszalek and Julio M. Fernandez

A dense network of interconnected proteins and carbohydrates forms the complex mechanical scaffold of living tissues. The recently developed technique of single molecule force spectroscopy using the atomic force microscope (AFM) has enabled a detailed analysis of the force-induced conformations of these molecules and the determinants of their mechanical stability. These studies provide some of the basic knowledge required to understand the mechanical interactions that define all biological organisms.

Mechanical stretching *in vivo* is thought to regulate the function of proteins, polysaccharides and DNA[1–6]. The application of mechanical force to biological polymers produces conformations that are different than those that have been investigated by chemical or thermal denaturation[7] and are inaccessible to conventional methods of measurement such as NMR spectroscopy and X-ray crystallography. Force-induced conformational transitions may therefore be physiologically relevant, and may offer novel perspectives on the structure of biomolecules. Recent developments in single molecule force spectroscopy have enabled studies of the mechanical properties of single biological polymers[8–14]. The force-measuring mode of the atomic force microscope (AFM) is capable of measuring force-induced domain unfolding in proteins[13,15–24], length transitions caused by conformational changes in the sugar rings[4,12,25,26] or in the secondary structure[27] of polysaccharides, and modifications of the secondary structure of DNA molecules[28,29]. A combination of the imaging and the force-measuring modes of the AFM has been used to extract single protein molecules from biological membranes[30,31] (see review by Engel and Müller[32] in this issue). The AFM may therefore help to elucidate the molecular determinants of mechanical stability and the role of force-induced conformational changes in the regulation of physiological function. This review will focus mostly on the use of the AFM to study the dynamic changes that proteins undergo in response to mechanical force.

The force spectroscopy mode of the AFM

In the force-measuring mode of the AFM, single molecules or pairs of interacting molecules are stretched between the tip of a microscopic cantilever and a flat, gold-covered substrate whose position is controlled by a high precision piezoelectric positioner (Fig. 1*b*). This system allows the suspended molecule(s) to be stretched with

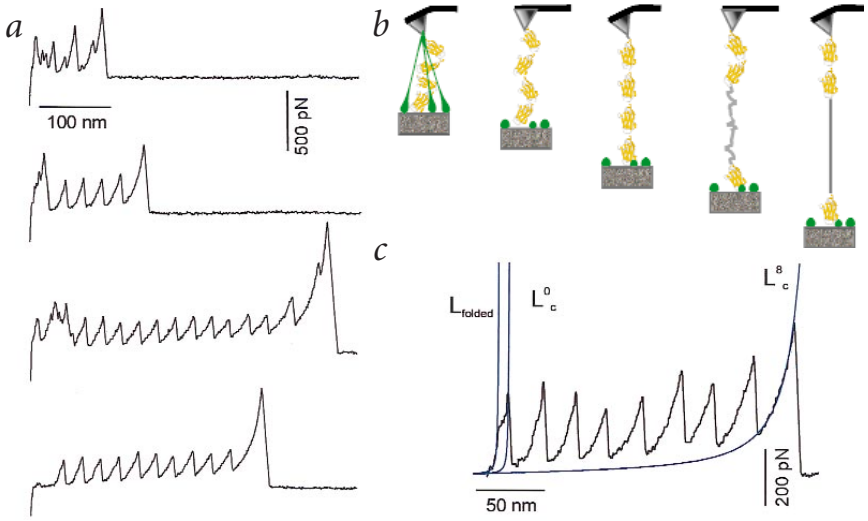

Fig. 1 The extension of modular proteins with the AFM. ***a***, A series of four force extension curves obtained from a pure sample of protein consisting of 12 identical domains. In each case the final peak represents extension of the completely unfolded protein and its detachment from either the cantilever or the gold substrate. Note that the pattern of force peaks prior to detachment in the first trace is irregular in amplitude and spacing and is therefore uninterpretable. In the subsequent traces, however, there are varying numbers of evenly spaced peaks of similar amplitude corresponding to the consecutive unfolding of the protein domains, with or without an early region of nonspecific interaction. ***b***, A schematic diagram of the progression of events during withdrawal of the gold substrate (gray box) during an AFM experiment. Prior to the experiment, a layer of proteins was allowed to adsorb to the gold substrate. Then the AFM cantilever (pyramidal tipped lever) is pressed against the protein layer to allow adsorption to the cantilever. Upon withdrawal of the gold substrate, the cantilever is first deflected by interactions with other molecules such as denatured protein (in green). When these interactions break, the force on the cantilever is released. As the modular protein is stretched, the force on the cantilever increases until one of the domains unravels causing the force on the cantilever to drop. The force begins to increase again when the unfolded domain is fully elongated. ***c***, The WLC model can be used to fit the force extension relationship of the protein following unfolding of all of the domains (L^8_c), or prior to any of the unfolding events (for example prior to the first domain unfolding, L^0_c). The first fit (L_{folded}) represents extension of the protein prior to the occurrence of an unfolding intermediate (see text and Fig. 2).

Department of Physiology and Biophysics, Mayo Foundation, 1-117 Medical Sciences Building, Rochester, Minnesota 55905, USA.

Correspondence should be addressed to J.M.F. *email: fernandez.julio@mayo.edu*

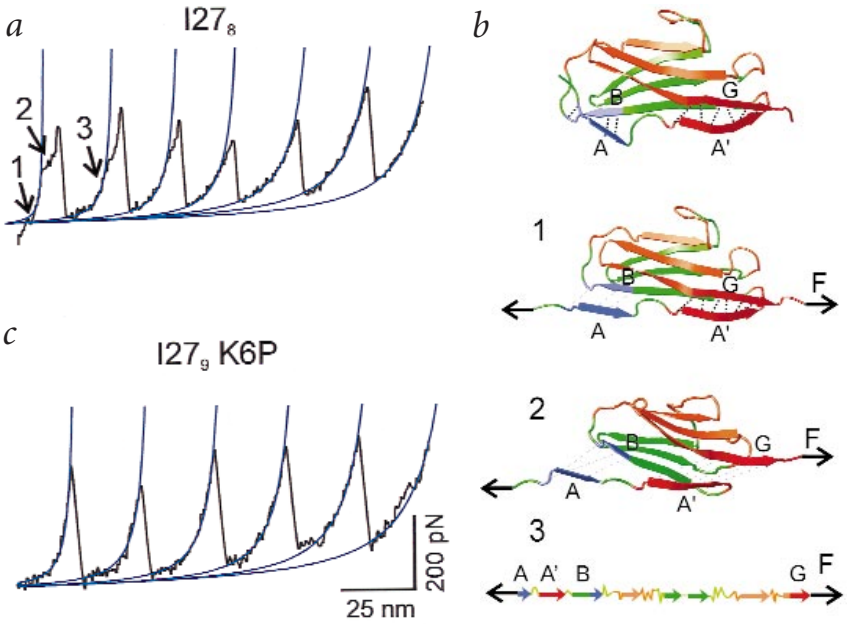

Fig. 2 Identification of an unfolding intermediate in the extension of I27 and the prevention of this intermediate by a point mutation. ***a***, Force extension curves for $I27_8$ (upper trace) and for the K6P mutant of $I27_9$ ($I27_9$-K6P, lower trace) showing fits of domain unfolding according to the WLC model (blue lines). Note that $I27_8$ shows a prominent hump in the rising phase of the initial force peaks, while no such humps are seen for $I27_9$-K6P. The numbers in the upper trace refer to the stages of extension of I27 pictured in (b). ***b***, Steered molecular dynamics simulations of the structure of I27 under no stress (upper diagram) (i) under some force showing extension of the bonds between the A and B strands (ii) under greater stress with the A–B bonds broken and the A′–G patch being extended and (iii) following complete unraveling of the domain (not drawn to scale). (Fig. 2*b* adapted from ref. 47 and generated using the program VMD[74]).

subnanometer precision. The forces acting on the molecule as it is extended are transmitted to the cantilever, causing it to bend. The amount of bending is measured by a laser beam reflected off the cantilever tip onto a photodetection system, such that the vertical deflection of the beam registers the angle at which the cantilever is bent[33–35]. By calibrating the responsiveness of the cantilever[36], the degree of bending can be translated into the applied force with a precision at the level of a few piconewtons (pN).

Interpretation of force extension relationships

The sensitivity of the AFM has enabled experiments to probe the mechanical properties of several types of native and engineered modular proteins[13,15–24]. In a typical experiment, the cantilever tip is pressed into a layer of purified protein adsorbed onto the gold substrate. Protein molecules from the adsorbed layer affix to the cantilever by an unknown mechanism (which could involve the high pressures achieved as the cantilever tip is pressed against the gold substrate[37]) and are stretched as the gold substrate is withdrawn. Suspended molecules resist extension and therefore cause deflection of the cantilever. The tension on the cantilever is released either when a force-induced rearrangement increases the distance between the ends of the suspended protein (culminating in the complete unraveling of the protein fold), or when the suspended molecule(s) become detached from the cantilever or gold substrate. The resultant data may be expressed as a force extension curve.

The traces in Fig. 1*a* represent force extension curves obtained from a sample of a protein composed of 12 identical domains. The final peak in each trace represents detachment of the final protein molecule(s). These traces demonstrate that even when a sample of a pure protein is used, spurious peaks may occur in the force extension curve because the protein molecule may have been completely or partially denatured due to interactions with the gold substrate or to entanglement with other protein molecules. Such interactions, which typically occur when the cantilever is within ~30–50 nm of the gold substrate, might yield a force extension relationship displaying a single force peak, or one displaying several peaks that are irregular in amplitude and spacing (Fig. 1*a*, uppermost trace). Mechanical interference of this kind may occur with any sample of biological polymer, and, although it could easily be mistaken for real data, is essentially uninterpretable. The presence of the regularly spaced, saw-tooth pattern of force peaks seen in the lower three traces in Fig. 1*a*, however, is the unmistakable fingerprint of a modular protein. These peaks correspond to the consecutive unfolding of each of the protein domains in a single protein molecule. As a molecule is elongated, the resistive force increases until one of the domains gives way and unravels, releasing the tension on the cantilever (Fig. 1*b*). Continued extension causes the resistive force to increase again until the next unfolding event occurs. Force extension curves can yield unfolding force peaks equal to the number of domains in the protein (as in trace 3 of Fig. 1*a*), but more frequently will yield fewer peaks or no peaks at all (as in trace 1 of Fig. 1*a*).

Analysis of the saw-tooth pattern

Analysis of saw-tooth patterns has provided quantitative information about the mechanical properties of different types of modular proteins[13,15–17]. One crucial characteristic of this pattern is that the amplitude at which an unfolding event occurs reflects the mechanical stability of the folded domain under the experimental conditions used. Unfolding is a probabilistic event that can occur at any force, and it therefore depends on the rate of extension, with higher force required to cause unfolding at greater rates of extension[38–41]. A second characteristic of the saw-tooth pattern is that the spacing between the peaks reflects the number of amino acids that each unfolding event adds to the total length. Domains of equal size should therefore yield evenly spaced peaks. Observation of such a pattern verifies that the data reflects the unfolding properties of the molecule of interest and allows quantitative analysis of the mechanical properties of the protein domains (Fig. 1*c*; see below).

Mechanical properties of a protein module

The heterogeneity of native proteins complicates the interpretation of AFM studies. When a modular protein containing multiple different domains is stretched, it is difficult to relate individual unfolding peaks in the force extension curve to specific domains, and therefore to determine the mechanical properties of a specific fold. The solution to this problem was found in molecular biology. By ligating multiple copies of the cDNA encoding a specific domain and expressing the resultant gene in bacteria, it has been possible to produce 'polyproteins' consisting of multiple copies of

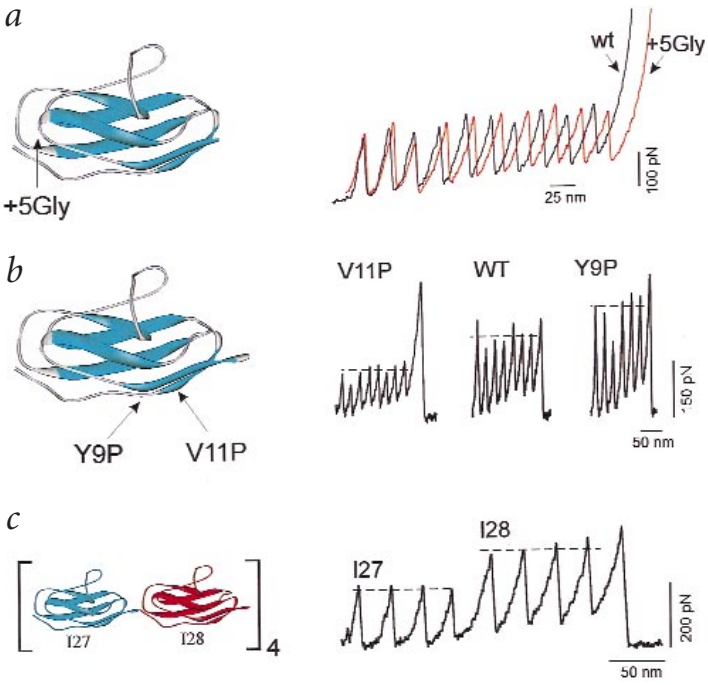

Fig. 3 The engineering of polyproteins to probe the structure of immunoglobulin domains. ***a***, Insertion of a cassette of five glycine molecules into the structure of I27 (model on the left) causes an increase in the interval between unfolding peaks observed with the AFM (traces on the right). The difference between the wild type polyprotein (wt) and that constructed from the glycine mutant (+5Gly) is ~2.0 nm, or ~0.4 nm per glycine residue. ***b***, Mutations of amino acids involved in the A′–G patch of the I27 domain can change the force required for unfolding. While the V11P mutant results in a decrease in the amplitude of unfolding force peaks, the Y9P mutant shows force peaks that are higher than the wild type I27 domain (WT). ***c***, A chimera constructed of repeats of I27 and I28 yields a force extension relationship demonstrating that the domains with lower mechanical stability (I27) unfold on average at lower forces, irrespective of the arrangement of the domains within the protein.

a single protein fold[22]. For example, a polyprotein consisting of eight copies of immunoglubulin domain 27 from human cardiac titin (referred to as $I27_8$) has allowed quantitative study of the mechanical properties of this domain. Extension of this polyprotein (Fig. 1*c*) yielded a force extension curve with evenly spaced peaks with an amplitude tightly clustered around a mean of 204 ± 26 pN (ref. 22).

The data obtained from the force extension curve from a engineered polyprotein may be analyzed quantitatively using models that describe the physics of polymer elasticity. Polymer chains that are free in solution exist in a coiled state since this maximizes their conformational freedom and therefore entropy. Extension of the molecule generates an opposing force due to the reduction in entropy, as the freedom of movement of the molecule is restricted. The behavior of polymers under stress may be predicted using the 'worm-like chain' model of entropic polymer elasticity (WLC[42–44]). The WLC uses the length and flexibility of a molecule to model how it would respond to forced extension.

The results of fitting three portions of a saw-tooth pattern are shown in Fig. 1*c*. The first fit (L_{folded}) represent the length of the protein prior to the unfolding of any domains, whereas the third fit represents the extension of the protein after all eight domains have been unfolded (L^8_c). Fitting the upswing of earlier peaks with the WLC theory (for example, the second fit L^0_c in Fig. 1*c*) gives the length of the protein prior to that particular unfolding event. The interval between events gives the increment due to unfolding. The distance between the extrapolated length of L^8_c and L^0_c, for example, indicates the increase in the length of the protein caused by unfolding all eight domains. The use of a polyprotein allows this interval to be estimated with great precision because it allows simultaneous fitting of multiple peaks. For $I27_8$, unfolding each domain adds 28.4 ± 0.3 nm to the length of the protein[22], which corresponds to a stretch of ~70 amino acids. This is less than the total number of amino acids in the fold (89), suggesting that interactions within the fold form a point of resistance that protects amino acids from mechanical stress, until the unfolding event occurs. Each domain therefore consists of 'force bearing' amino acids, which are exposed to stress prior to the unfolding event, and 'hidden' amino acids, which are stretched only after unfolding occurs. The number of hidden amino acids in the I27 domain suggests that there is a critical point of mechanical resistance between two parts of the I27 sequence that differ by ~70 amino acids. This hypothesis is in good agreement with the calculations made by Klaus Schulten and collaborators who used steered molecular dynamics simulations[45] to predict the atomic events during the force-induced unfolding of the I27 module. These simulations showed that the A′–G contact region contains several hydrogen bonds that must be broken simultaneously for the relative motion of the two strands to occur (Fig. 2*b*)[46,47]. Inspection of the structure of the I27 domain (Fig. 2*b*) shows that ~70 amino acids are 'sequestered' by the A′–G contact region, in excellent agreement with our observations.

Comparing chemical and AFM protein unfolding

Extrapolation of the rates of unfolding measured at different forces allows estimation of the rate of unfolding at zero force. This permits a comparison with estimates of spontaneous unfolding rates derived from chemical denaturation experiments. The rates of spontaneous unfolding for an I27 domain estimated in these ways are strikingly similar (4.9×10^{-4} s^{-1} and 3.3×10^{-4} s^{-1} for chemical and mechanical experiments, respectively). This similarity suggests that breaking the A′–G interactions might be the rate-determining step of spontaneous unfolding, and that chemical or mechanical denaturation requires disruption of these interactions.

Recent molecular dynamics (MD) simulations by Paci and Karplus[48] suggest, however, that force-induced unfolding may occur through a distinct pathway. While the A′–G strands must dissociate before mechanical stress alters the structure within the folded domain, thermal denaturation causes disruption of interactions throughout the domain prior to disruption of the A′–G contacts. Furthermore, the same simulation study indicates that mechanical unfolding after breaking the A′–G interactions produces conformations that do not occur during thermal denaturation[48]. The presence of critical interactions acting as molecular thresholds to forced unfolding may be a property of domains that are exposed to mechanical force. Such interactions may protect domains from unfolding at low force, but allow for force-induced rupture at higher forces.

Identification of an unfolding intermediate

The force extension curves of I27 polyproteins reveals an intermediate conformation that occurs at forces lower than that required to cause full domain unfolding[19]. This intermediate is manifested by a deviation from the expected WLC behavior (Fig. 2*a*; blue lines) prior to the first unfolding peak (the 'hump') and by progressively smaller deviations prior to subsequent peaks (Fig. 2*a*). Molecular

simulations suggest that this corresponds to a lengthening of each domain (by ~15%) as the hydrogen bonds linking the A and B strands are broken, allowing additional amino acids to become force-bearing (Fig. 2*b*). The size of each subsequent hump is proportional to the number of unfolding events yet to occur, suggesting that upon relaxation the A and B strands in domains that remain folded rapidly reconnect. The A–B interactions thus form a hinge-like mechanism to regulate the length of an I27 domain in response to moderate levels of mechanical force. Such an intermediate would be difficult to detect using methods other than AFM because it occurs when the molecule is under mechanical stress and because it is not associated with unfolding of the hydrophobic core of the domain.

Mutagenesis studies of the I27 polyprotein

An important benefit of using engineered polyproteins for AFM studies is that they can be constructed from domains with an altered amino acid sequence, thereby allowing dissection of the molecular determinants of mechanical stability. Mutations were used to test the hypothesis that the intermediate described in the previous section is due to the interactions between A and B strands. Substituting a proline for a lysine at position 6, which forms part of this interaction interface, completely abolishes the hump (Fig. 2*a,* lower trace)[19]. This observation provides strong support to the hypothesis that it is the disruption of the A–B interactions that causes the conformational change underlying the hump.

Insertions of amino acids into a domain can be used to probe the mechanical topology of this domain. For example, insertion of a cassette of five glycines at a position near one of the ends of the I27 sequence that is predicted to be part of the force-bearing amino acids had no effect on the interval between unfolding peaks. In contrast, insertion of the same cassette into a sequence predicted to be inside the folded domain increased the interval between unfolding events by ~2.0 nm (Fig. 3*a*)[23].

Recent data show that point mutations within the region underlying the barrier to mechanical unfolding can dramatically alter the force required for unfolding (Fig. 3*b*) (H. Li, M. Carrion-Vazquez, A.F. Oberhauser, P.E.M. & J.M.F. unpublished results). Amino acids in the A′ strand were replaced with prolines to prevent the formation of hydrogen bonds with the G strand. As expected, mutation of valines to prolines at positions 11, 13 and 15 decreased the force required for domain unfolding. Mutation of tyrosine to proline at position 9, however, actually increased the mechanical stability of the domain. These observations demonstrate the utility of combining mutagenesis with engineered polyproteins to elucidate the molecular interactions underlying mechanical stability.

A polyprotein chimera

Ig domains have different mechanic stabilities that can easily be differentiated by the AFM. For example, the Ig domain that follows I27 in human cardiac titin (I28) has a mean unfolding force of 257 ± 27 pN (ref. 20). When a polyprotein consisting of repeating units of I27-I28 dimers was stretched, the I27 domains unfolded before the first I28 domain did (Fig. 3*c*)[20]. This demonstrates that the order of domain unfolding of a modular protein is unrelated to the arrangement of its constituent domains; rather, it is determined by their intrinsic mechanical stability.

Refolding after mechanical unfolding

Mechanically induced unfolding puts proteins into conformations that are not observed in chemical denaturation studies, but which may occur *in vivo* — the extended denatured state. The different ensemble of conformations in the extended denatured state implies different energetics of refolding from this state. When the protein is fully extended, its freedom of motion, and therefore entropy, is minimal. After the tension on the molecule is released, the entropy of the molecule rapidly increases, driving the molecule into a compact conformation that may correspond to the molten globule state described in models of protein folding[49–51]. This state may be the point of maximal entropy during the refolding process. When the polypeptide returns to its native conformation the entropy is again minimized.

Using an AFM it is possible to extend a protein such that it is fully unfolded but does not detach from the cantilever tip. Tension on the protein may then be relaxed by returning the tip and gold substrate to their positions before unfolding. In this position the domains of the protein can actually refold, allowing the protein to undergo forced unfolding again.

By varying the interval between relaxation and re-extension, the refolding rates of domains within a polyprotein could be measured. I27 domains in a polyprotein refold with a single exponential rate of 1.2 s^{-1} (ref. 22). The fidelity of refolding after a mechanical extension is remarkable. Misfolding events, where the A′ strand of one I27 domain interacts with the G strand of another domain, do occur, but are rare (only ~2% of events)[18].

Polysaccharides under a stretching force

Polysaccharides play critical roles in cell adhesion and are responsible for the mechanical integrity of bacterial and plant cell walls. Recently, the AFM has been used to characterize the elasticity of single polysaccharide molecules[4,12,25–27]. Polysaccharides whose glycosidic linkages are attached equatorially to the pyranose ring (for example, cellulose) were found to follow the freely jointed chain (FJC) model of polymer elasticity[4,27]. However, polysaccharides with axial linkages, such as dextran, amylose and pectin, were found to undergo abrupt force-induced length transitions[4,12,25,26]. These transitions are caused by the shift of individual pyranose rings from the chair conformation to the boat or the inverted chair conformations which, as corroborated by *ab initio* calculations, provide an increased distance between glycosidic bonds[4,25]. The AFM results contrast the view that sugars are inelastic and locked into a stable conformation, raising the tantalizing possibility that force-driven sugar conformations play important roles in biological signaling[4] as well as in the elasticity of polysaccharides[12,25].

Force spectroscopy of DNA

Tension on a DNA molecule is thought to be a critical component regulating the activity of a variety of DNA enzymes including polymerases during their transcription work[6,52] and topoisomerases when they untangle DNA[53]. The mechanical properties of a relaxed and supercoiled DNA have been explored using a variety of techniques, including laser tweezers[5,6,9,52], hydrodynamic flow gradients[54], a receding meniscus[55], micro fibers[10,56], magnetic beads[8,53,57] and, last but not least, the AFM[28,29]. These experiments were accompanied by theoretical work to explain the complex nature of elasticity of a double stranded and single stranded DNA[8–10,43,44,58–61]. While an extension of single stranded DNA (ssDNA) molecules conforms to the FJC model supplemented with the segment elasticity[9], stretching of a double stranded DNA (dsDNA) results in an extensive conformational change of the molecule that occurs at a critical force of ~65 pN (refs 9,10,28). At this tension DNA undergoes a highly cooperative transition to an overstretched conformation called the 'S' DNA — it is characterized by a 5.8 Å rise per base pair[9] that is 70% longer than B-form dsDNA[9,10,55,62]. Because the B-S transition may be part of the homologous recombination process[5,56], the overstretched state of DNA by AFM could be of con-

siderable interest. These observations have been recently reviewed by Bustamante and colleagues[63].

In addition to measuring the mechanical properties of a DNA molecule, force spectroscopy on nucleic acids has other applications. Essevaz-Roulet *et al.*[64] used a glass microneedle to separate the complementary strands of a single DNA molecule. Interestingly, the force spectrographs obtained from these experiments were sequence-dependent and predicted a rupture force of ~15 pN for the G-C base pairs and 10 pN for the A-T base pairs. Gaub and collaborators more recently used an AFM to stretch double stranded DNA molecules[28]. The AFM, when compared with other force probes, can make measurements on shorter molecules while exerting forces of greater magnitude, thereby extending the information obtained through force spectrographs. In these measurements overstretching was followed by a second transition at a higher force (~150 pN), corresponding to the melting of double stranded DNA into single strands[28,29]. Furthermore, the melted ssDNA was observed to form hairpins that could be unraveled at a force that was sequence specific and that agreed closely with the results of Essevaz-Roulet *et al.*[64]. These results thus open up the possibility of mechanically reading out the sequence of a single DNA molecule, with large implications for the field of genomics. However, this appealing goal is still elusive due to the relatively low resolution of the probes used.

Perspective

The AFM can stretch biopolymers into important conformations that are inaccessible to other methods of measurement. Therefore, the AFM promises to become an important tool for understanding the micromechanics of living tissues. The AFM instrumentation is continuously improving. For example, recent efforts in the laboratory of Paul Hansma have focused on developing a high speed AFM (~100 kHz bandwidth) that can read out small forces (~1 pN)[65]. This has already proven to be useful in monitoring protein–protein interactions in real time[66]. AFM probes made of single carbon nanotubes now promise to combine probe chemistry with highly localized mechanical contacts[67]. Thus, it is reasonable to expect that AFM techniques will soon be able to monitor a wide range of single molecule chemical reactions.

The force-driven conformations of biological polymers have wide implications. Proteins in both animals and plants are frequently anchored in two or more locations and are therefore exposed to mechanical stress due to tissue strain, and experience changes in stress during movement, development, and morphological plasticity. Mechanically stressed proteins are frequently modular structures composed of multiple individually folded β-sandwich domains of the immunoglobulin (Ig), fibronectin, cadherin types[68]. There is accumulating evidence that partial or complete unfolding of such domains *in situ* allows proteins to undergo graded increases in length and may regulate the activity of specific domains. For example, the extracellular matrix (ECM) protein fibronectin is thought to contain a domain that must unfold to enable self-association of fibronectin fibrils[2,69–72]. These new forms of mechanical signaling may not be restricted to proteins. For example, the binding of polysaccharides to ECM proteins may depend also on force driven-conformations of its constituent sugars[4]. The mechanical manipulations of single DNA molecules have proven to be very revealing. DNA function was found to be intimately related to its local strain and stress (see above), and the force spectroscopy experiments have uncovered new mechanical conformations that are different from those found in proteins and polysaccharides (for example, the overstretching transition).

Force spectroscopy has become a powerful tool for studying the force-driven conformations of proteins, polysaccharides and nucleic acids, and could provide new insights into the basic micromechanical architecture of biological systems. The applications of this technique on engineered biopolymers and fibers with novel mechanical properties would likely initiate the discovery of new materials[20,73]. Force spectroscopy is thus a versatile tool in both structural biology and material sciences.

Acknowledgment

We thank A. Oberhauser, M. Carrion-Vazquez and H. Li for ideas, data and figures for this review and K. Schulten for the images in Fig. 2*b*.

Received 9 June, 2000; accepted 3 August, 2000.

1. Erickson, H.P. *Proc. Natl. Acad. Sci. USA* **91**, 10114–10118 (1994).
2. Zhong, C. *et al. J. Cell. Biol.* **141**, 539–551 (1998).
3. Shaub, A. *Nature Cell. Biol.* **1**, E173–E175 (1999).
4. Marszalek, P.E. *et al. Proc. Natl. Acad. Sci. USA* **96**, 7894–7898 (1999).
5. Hegner, M., Smith, S.B. & Bustamante, C. *Proc. Natl. Acad. Sci. USA* **96**, 10109–10114 (1999).
6. Wuite, G.J., Smith, S.B., Young, M., Keller, D. & Bustamante, C. *Nature* **404**, 103–106 (2000).
7. Fisher, T.E., Oberhauser, A.F., Carrion–Vazquez, M., Marszalek, P.E. & Fernandez, J.M. *Trends Biochem. Sci.* **24**, 379–384 (1999).
8. Smith, S.B., Finzi, L. & Bustamante, C. *Science* **258**, 1122–1136 (1992).
9. Smith, S.B., Cui, Y. & Bustamante, C. *Science* **271**, 795–799 (1996).
10. Cluzel, P. *et al. Science* **271**, 792–794 (1996).
11. Tskhovrebova, L., Trinick, J., Sleep, J.A. & Simmons, R.M. *Nature* **387**, 308–312 (1997).
12. Rief, M., Oesterhelt, F., Heymann, B. & Gaub, H.E. *Science* **275**, 1295–1297 (1997).
13. Rief, M., Gautel, M., Oesterhelt, F., Fernandez, J.M. & Gaub, H.E *Science* **276**, 1109–1112 (1997).
14. Kellermayer, M.S., Smith, S.B., Granzier, H.L. & Bustamante, C. *Science* **276**, 1112–1116 (1997).
15. Rief, M., Gautel, M., Schemmel, A. & Gaub, H.E. *Biophys. J.* **75**, 3008–3014 (1998).
16. Rief, M., Pascual, J., Saraste, M. & Gaub, H.E. *J. Mol. Biol.* **286**, 553–561 (1999).
17. Oberhauser, A.F., Marszalek, P.E., Erickson, H.P. & Fernandez, J.M. *Nature* **393**, 181–185 (1998).
18. Oberhauser, A.F., Marszalek, P.E., Carrion-Vazquez, M. & Fernandez, J.M. *Nature Struct. Biol.* **6**, 1025–1028 (1999).
19. Marszalek, P. E. *et al. Nature* **402**, 100–103 (1999).
20. Li, H., Oberhauser, A.F., Fowler, S. B., Clarke, J. & Fernandez, J.M. *Proc. Natl. Acad. Sci. USA* **97**, 6527–6531 (2000).
21. Yang, G. et al. Proc. Natl. Acad. Sci. USA **97**, 139–144 (2000).
22. Carrion-Vazquez, M. *et al. Proc. Natl. Acad. Sci. USA* **96**, 3694–3699 (1999).
23. Carrion-Vazquez, M., Marszalek, P.E., Oberhauser, A.F. & Fernandez, J.M. *Proc. Natl. Acad. Sci. USA* **96**, 11288–11292 (1999).
24. Carrion-Vazquez, M. *et al. Progress in biophysics and molecular biology* **in the press** (2000).
25. Marszalek, P.E., Oberhauser, A.F., Pang, Y.P. & Fernandez, J.M. *Nature* **396**, 661–664 (1998).
26. Li, H. *et al. Chem. Phys. Lett.* **305**, 197–201 (1999).
27. Li, H., Rief, M., Oesterhelt, F. & Gaub, H.E. *Adv. Materials* **3**, 316–319 (1998).
28. Rief, M., Clausen-Schaumann, H. & Gaub, H.E. *Nature Struct. Biol.* **6**, 346–349 (1999).
29. Clausen-Schaumann, H., Rief, M., Tolksdorf, C. & Gaub, H.E. *Biophys. J.* **78**, 1997–2007 (2000).
30. Müller, D.J., Baumeister, W. & Engel, A. *Proc. Natl. Acad. Sci. USA* **96**, 13170–13174 (1999).
31. Oesterhelt, F. *et al. Science* **288**, 143–146 (2000).
32. Engel, A. & Müller, D.J. *Nature Struct. Biol.* **7**, 715–718 (2000).
33. Amer, N.M. & Meyer, G. *Bull. Am. Phys. Soc.* **33**, 319 (1988).
34. Meyer, G. & Amer, N.M. *Appl. Phys. Lett.* **53**, 1045–1047 (1988).
35. Alexander, S. *et al. J. Appl. Phys.* **65**, 164–167 (1989).
36. Florin, E.L. et al. Biosensors and Bioelectronics **10**, 895–901 (1995).
37. van Eldik, R. & Hubbard, C.D. *Chemistry under extreme or non-classical conditions* (Wiley; Spektrum, New York; 1997).
38. Bell, G.I. *Science* **200**, 618–27 (1978).
39. Alon, R., Hammer, D.A. & Springer, T.A. *Nature* **374**, 539–542 (1995).
40. Merkel, R., Nassoy, P., Leung, A., Ritchie, K. & Evans, E. *Nature* **397**, 50–53 (1999).
41. Evans, E. *Faraday Discussions* **111**, 1–16 (1998).
42. Flory, P. J. *Statistical mechanics of chain molecules* (Hanser Publishers ; Distributed in the U.S.A. by Oxford University Press, Munich ; New York, New York; 1988).
43. Bustamante, C., Marko, J.F., Siggia, E.D. & Smith, S. *Science* **265**, 1599–1600 (1994).
44. Marko, J.F. & Siggia, E.D. *Macromolecules* **28**, 8759–8770 (1995).
45. Lu, H. & Schulten, K. *Proteins Struct. Funct. Genet.* **35**, 453–463 (1999).
46. Lu, H., Isralewitz, B., Krammer, A., Vogel, V. & Schulten, K. *Biophys. J.* **75**, 662–671 (1998).
47. Lu, H. & Schulten, K. *Biophys. J.* **79**, 51–65 (2000).
48. Paci, E. & Karplus, M. *Proc. Natl. Acad. Sci. USA* **97** 6521–6526 (2000).
49. Onuchic, J.N., Luthey-Schulten, Z. & Wolynes, P.G. . *Annu. Rev. Phys. Chem.* **48**, 545–600 (1997).
50. Chan, H.S. & Dill, K.A. *Proteins* **30**, 2–33 (1998).
51. Matagne, A. & Dobson, C.M. *Cellular and Molecular Life Sciences* **54**, 363–371 (1998).
52. Davenport, R.J., Wuite, G.J., Landick, R. & Bustamante, C. *Science* **287**, 2497–2500 (2000).

53. Strick, T.R., Croquette, V. & Bensimon, D. *Nature* **404**, 901–904 (2000).
54. Perkins, T.T., Smith, D.E. & Chu, S. *Science* **276**, 2016–2021 (1997).
55. Bensimon, D., Simon, A.J., Croquette, V. & Bensimon, A. *Phys. Rev. Lett.* **74**, 4754–4757 (1995).
56. Leger, J.F., Robert, J., Bourdieu, L., Chatenay, D. & Marko, J.F. *Proc. Natl. Acad. Sci. USA* **95**, 12295–12299 (1998).
57. Strick, T.R., Allemand, J.-F., Bensimon, D., Bensimon, A. & Croquette, V. *Science* 271, 1835–1837 (1996).
58. Vologodskii, A. *Macromol.* **27**, 5623–5625 (1994).
59. Marko, J.F. & Siggia, E.D. *Science* **265**, 506–508 (1994).
60. Odijk, T. *Macromol.* **28**, 7016–7018 (1995).
61. Bouchiat C., Wang, M.D., Allemand, J.F., Strick, T., Block, S.M. & Croquette, V. *Biophys. J.* **76**, 409–413 (1999).
62. Ahsan, A., Rudnick, J. & Bruinsma, R. *Biophys. J.* **74**, 132–137 (1998).
63. Bustamante, C., Smith, S.B., Liphardt, J. & Smith, D. *Curr. Opin. Struct. Biol.* **10**, 279–285 (2000).
64. Essevaz-Roulet, B., Bockelmann, U. & Heslot, F. *Proc. Natl. Acad. Sci. USA* **94**, 11935–11940 (1997).
65. Viani, M.B. *et al. Rev. Sci. Instru.* **70**, 1–4 (1999).
66. Viani, M.B. *et al. Nature Struct. Biol.* 7, 644–647 (2000).
67. Wong, S. S., Joselevich, E., Woolley, A. T., Cheung, C. L. & Lieber, C. M. *Nature* **394**, 52–5 (1998).
68. Fisher, T. E. *et al. Neuron* (2000) **in the press**.
69. Hocking, D.C., Sottile, J. & McKeown-Longo, P.J. *J. Biol. Chem.* **269**, 19183–19187 (1994).
70. Morla, A., Zhang, Z. & Ruoslahti, E. *Nature* **367**, 193–196 (1994).
71. Ingham, K.C., Brew, S.A., Huff, S. & Litvinovich, S.V. *J. Biol. Chem.* **272**, 1718–1724 (1997).
72. Ohashi, T., Kiehart, D.P. & Erickson, H.P. *Proc. Natl. Acad. Sci. USA* **96**, 2153–2158 (1999).
73. Smith, B.L. *et al. Nature* **399**, 761–763 (1999).
74. Humphrey, W., Dalke, A., & Schulten, K. *J. Mol. Graphics*, 14, 33–38 (1996).

Measuring conformational dynamics of biomolecules by single molecule fluorescence spectroscopy

Shimon Weiss

Dynamic structural changes of macromolecules undergoing biochemical reactions can be studied using novel single molecule spectroscopy tools. Recent advances in applying such distance and orientation molecular rulers to biological systems are reviewed, and future prospects and challenges are discussed.

The field of single molecule spectroscopy (SMS) has grown rapidly in recent years. The ability to watch one molecule at a time helps us obtain unique information on distribution functions of relevant observables, resolve subpopulations in a heterogeneous sample and record asynchronous time trajectories of observables that would otherwise be hidden during biochemical reactions. We are past the first round of methodology development and validation of techniques — we no longer ask if single molecule studies can teach us more than ensemble measurements; rather, we ask what new biology will be unraveled. Indeed, the enthusiastic acceptance and quick adaptation of SMS by many investigators in the life sciences clearly manifest its great promise and the high level of expectations for new discoveries resulting from it.

This brief review does not intend to give a comprehensive historical account or a detailed analysis of various SMS methodologies[1–9]. Rather, it focuses on very recent developments in 'dynamic structural biology' using fluorescent tags as the means to monitor conformational changes (distance and orientation) of biological macromolecules. The discussion is limited to SMS methods that take advantage of two unique properties of single fluorophores — their very high sensitivity to the presence of other nearby fluorophores and quenchers; and their unique absorption and emission transition dipoles, which provide information on rotational freedom of motion and changes in orientation. Here we describe how distance changes between two sites on a macromolecule (or between two different molecules) can be measured *via* single pair fluorescence resonance energy transfer (spFRET) and how changes in orientation can be detected by measuring the changes in the dipole orientation of a rigidly attached probe or a tethered probe *via* single molecule fluorescence polarization anisotropy (smFPA).

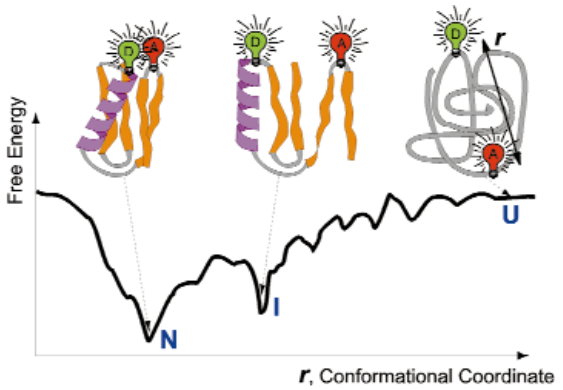

Fig. 1 Energy landscape for the folding reaction. A cartoon of free energy as a function of distance r between the fluorescence donor and acceptor. The rugged energy landscape has a funnel shape. U, the unfolded state; I, an intermediate state; N, the folded state.

In the past two years several groups successfully applied spFRET and smFPA to single molecule enzymology and macromolecule folding reactions. These exciting new results are reviewed and future challenges and prospects are discussed.

Materials Sciences and Physical Biosciences Divisions, Lawrence Berkeley National Laboratory, Berkeley, California 94720, USA.

Correspondence should be addressed to S.W. *email: sweiss@lbl.gov*